THE JOURNAL OF BIOLOGICAL CHEMISTRY
Vol. 277, No. 1, Issue of January 4, pp. 295–302, 2002
Printed in U.S.A.

Mechanistic Studies with Potent and Selective Inducible Nitric-oxide Synthase Dimerization Inhibitors*

Received for publication, June 20, 2001, and in revised form, October 26, 2001
Published, JBC Papers in Press, October 31, 2001, DOI 10.1074/jbc.M105691200

Eric Blasko,[a] Charles B. Glaser,[b] James J. Devlin,[b] Wei Xia,[b] Richard I. Feldman,[c] Mark A. Polokoff,[d] Gary B. Phillips,[d] Marc Whitlow,[e] Douglas S. Auld,[f] Kirk McMillan,[f,g] Sanjay Ghosh,[h,i] Dennis J. Stuehr,[h,i] and John F. Parkinson[j,k]

From the [a]Cardiovascular Research, [b]Protein Expression and Cell Sciences, [c]Cancer Research, [d]Discovery Research, [e]Biophysics, and [j]Immunology Departments, Berlex Biosciences, Richmond, California 94804-0099, the [h]Lerner Research Institute, Cleveland Clinic, Cleveland, Ohio 44195, and [f]Pharmacopeia Inc., Princeton, New Jersey 08512

A series of potent and selective inducible nitric-oxide synthase (iNOS) inhibitors was shown to prevent iNOS dimerization in cells and inhibit iNOS *in vivo*. These inhibitors are now shown to block dimerization of purified human iNOS monomers. A ^{3}H-labeled inhibitor bound to full-length human iNOS monomer with apparent K_d ~1.8 nM and had a slow off rate, 1.2×10^{-4} s^{-1}. Inhibitors also bound with high affinity to both murine full-length and murine oxygenase domain iNOS monomers. Spectroscopy and competition binding with imidazole confirmed an inhibitor-heme interaction. Inhibitor affinity in the binding assay (apparent K_d values from 330 pM to 27 nM) correlated with potency in a cell-based iNOS assay (IC_{50} values from 290 pM to 270 nM). Inhibitor potency in cells was not prevented by medium supplementation with L-arginine or sepiapterin, but inhibition decreased with time of addition after cytokine stimulation. The results are consistent with a mechanism whereby inhibitors bind to a heme-containing iNOS monomer species to form an inactive iNOS monomer-heme-inhibitor complex in a pterin- and L-arginine-independent manner. The selectivity for inhibiting dimerization of iNOS *versus* endothelial and neuronal NOS suggests that the energetics and kinetics of monomer-dimer equilibria are substantially different for the mammalian NOS isoforms. These inhibitors provide new research tools to explore these processes.

The mammalian nitric-oxide synthase (NOS)[1] family consists of three isoforms as follows: cytokine-inducible (iNOS), neuronal (nNOS), and endothelial NOS (eNOS). NOS isoforms are homodimers that catalyze NADPH-dependent oxidation of L-arginine to nitric oxide (NO) and L-citrulline (1–3). Each monomer subunit of the dimer consists of a C-terminal reductase domain that contains binding sites for NADPH, FAD, FMN, and calmodulin, and an N-terminal oxygenase domain that contains binding sites for heme, tetrahydrobiopterin (H_4B), and L-arginine (3–7). As in cytochrome P-450, the NOS heme iron coordinates to the protein through a cysteine thiolate (6–8), binds O_2 as a sixth ligand (9), and participates directly in catalysis (9–13). The heme ligands CO, $^-$CN, imidazole, *N*-phenylimidazoles, and other imidazole-containing compounds all inhibit NO synthesis (10, 14–17).

The NOS isoforms are only active as homodimers (18–20). For iNOS (5) and nNOS (21–23), only the oxygenase domains of two monomers interact to form the dimer (24). Dimerization of iNOS is required for fully coupled enzyme activity because the flow of electrons during catalysis occurs in *trans* from the reductase domain of one monomer to the oxygenase domain of the other monomer (25). Dimerization of NOS monomers is initiated by heme insertion, which results in rapid conformational changes (18, 19, 26). The heme-containing iNOS monomer is an intermediate in dimerization and, in the presence of H_4B and L-arginine, forms a stable active dimer (18, 24, 27–29).

Highly potent and selective pyrimidineimidazole-based iNOS dimerization inhibitors were discovered via a combinatorial chemistry approach using a cell-based iNOS assay (30). Crystallographic studies showed that the inhibitors coordinate the heme in the iNOS monomer, disrupt helix 7a, and displace the critical arginine-binding Glu-371 residue from the active site. In addition helix 8, which is part of the dimer interface, is partially disordered by inhibitor binding. These results suggest that inhibitor binding to iNOS monomer prevents formation of both arginine- and H_4B-binding sites and leads to the formation of a "dead-end" inhibitor-monomer complex.

Interestingly, although the inhibitors led to accumulation of iNOS monomers in cells, they did not inhibit the catalytic activity of isolated dimeric iNOS. In the present study, biochemical characterization of these inhibitors with isolated human and murine iNOS monomers is presented. In addition, the binding kinetics of these inhibitors to iNOS monomers was determined using a high affinity radiolabeled inhibitor in a rapid filtration binding assay. Binding affinity in this assay correlated with inhibitory potency in cell culture. The results provide further insights into the mechanism of action of these novel inhibitors and introduce new reagents to study iNOS monomer-dimer equilibria.

EXPERIMENTAL PROCEDURES

Materials—Compounds were prepared as described previously (30). Recombinant full-length human iNOS monomer with an N-terminal six-histidine tag was expressed in a vaccinia virus-HeLa cell system and isolated using nickel-nitrilotriacetic acid and Superdex 200 chromatography as described previously (30). All purification steps were

* The costs of publication of this article were defrayed in part by the payment of page charges. This article must therefore be hereby marked "*advertisement*" in accordance with 18 U.S.C. Section 1734 solely to indicate this fact.

[g] Current address: Exelixis Inc., 170 Harbor Way, P.O. Box 511, South San Francisco, CA 94083-0511.

[i] Supported by National Institutes of Health Grant CA53914.

[k] To whom correspondence should be addressed: Immunology Dept., Berlex Biosciences, 15049 San Pablo Ave, Richmond, CA 94804-0099. Tel.: 510-669-4145; Fax: 510-669-4244; E-mail: john_parkinson@berlex.com.

[1] The abbreviations used are: NOS, nitric-oxide synthase; iNOS, inducible NOS; eNOS, endothelial NOS; nNOS, neuronal NOS; iNOS-ox, inducible NOS oxygenase domain; NO, nitric oxide; Δ114-iNOS-ox, murine iNOS oxygenase domain monomer with an N-terminal 114-residue deletion; H_4B, (6*R*)-5,6,7,8-tetrahydro-L-biopterin; PVDF, poly(vinylidene difluoride); Bistris, 2-[bis(2-hydroxyethyl)amino]-2-(hydroxymethyl)propane-1,3-diol.

performed at 4 °C, and the purified monomer was stored frozen at −80 °C. Full-length murine iNOS monomer, used for spectral studies, was prepared by urea dissociation of dimeric iNOS isolated from RAW 264.7 murine macrophage cells as described (29). Monomeric murine iNOS oxygenase domain with a 114-amino acid N-terminal deletion (Δ114-iNOS-ox) was expressed in *Escherichia coli* and prepared as described (32). All monomer preparations were >95% monomeric as determined by gel filtration chromatography (see for example Fig. 2*B, panel 1*).

Bistris propane, arginine, hemin chloride, sodium nitrite, sulfanilamide, *N*-(1-naphthyl)ethylenediamine, phosphoric acid, lactate (lactic) dehydrogenase, and sodium pyruvate were from Sigma. (*6R*)-5,6,7,8-Tetrahydrobiopterin was from Research Biochemicals International (Natick, MA). Reduced glutathione was from Fluka Chemical Co. (Milwaukee, WI). Hog brain calmodulin was from Roche Molecular Biochemicals. *N*-Succinimidyl [2,3-^{3}H]propionate and Superdex 200 gel filtration columns were purchased from Amersham Biosciences. Deep 96-well assay plates were from Beckman Instruments (Fullerton, CA). 96-Well filter plates containing poly(vinylidene difluoride) (PVDF) membranes were from Millipore (Bedford, MA; catalog number MAIP N0B). The C_{18} HPLC column was from Column Engineering (Ontario, Canada). The Speed Vac Concentrator was purchased from Savant (Holbrook, NY).

Protein Assay and Heme Content of iNOS Monomer Preparations—The protein content of purified NOS monomer preparations was determined using the method of Bradford according to the manufacturer's instructions (Bio-Rad) using bovine serum albumin as standard. The heme content of purified full-length human iNOS monomer preparations was determined spectrally by comparing the absorbance changes due to arginine or imidazole binding with that of pure human iNOS oxygenase domain (iNOSox) which had its heme content determined by the reduced pyridine hemochrome assay and by Soret band intensity upon binding of carbon monoxide (33). Dimeric iNOSox preparations that had a concentration of 10 μM heme-bound protein showed an increase at 400 nm and a decrease at 428 nm when excess arginine (1 mM) was added to imidazole-bound material (imidazole was first added to 0.25 mM). This difference or A_{400}–A_{428} was 0.40 OD units for 10 μM iNOSox. 2.58 μM full-length human iNOS monomer preparations had an A_{400}–A_{428} value of 0.010 OD units under the same conditions; hence the heme content was 0.25 μM, or about 10%. Using the A_{400}–A_{428} difference gave a more reliable measurement of heme content than absolute A_{428} for the human iNOS monomer preparations due to their low heme content and interference from bound flavins.

The heme content of murine iNOS monomer preparations was measured using the absorbance (corrected for light scattering) at 428 nm of imidazole-bound enzyme. By using this method, in which an A_{428} value of 0.48 was measured for 10 μM heme in dimeric iNOSox, the heme content of full-length murine iNOS monomer, which was prepared by the dissociation of dimeric iNOS by urea, was about 95% and of mouse Δ114-iNOS-ox monomer was about 85%.

iNOS Dimerization Assay—Dimerization of purified human iNOS monomer was performed by incubating the protein (0.6 μM) in NOS assay buffer (40 mM Bistris propane, 4 μM FAD, 4 μM FMN, 4 μM H_4B, 5 mM reduced glutathione, pH 7.8) containing 5 mM arginine, with or without 1.2 μM calmodulin and/or 0.6 μM hemin chloride as noted under "Results." The mixture was incubated for 2.5 h at 37 °C or at various time points as described under "Results." Compound **2** (2 μM) was added just prior to initiation of dimerization. For the experiment in Fig. 2*C*, the assay buffer also included 0.05 mg/ml bovine serum albumin and 0.01% Triton X-100 to prevent adsorption of protein on polypropylene surfaces. After the 2.5-h incubation, NO synthesis was measured using the colorimetric Griess assay for nitrite (34), as follows. Additional arginine (0.75 mM final concentration) and NADPH (1 mM final concentration) were added. After incubation for 30 min at 37 °C, the reaction was stopped by the addition of lactate dehydrogenase (60 units/ml) and 66 mM sodium pyruvate followed by incubation for 15 min at room temperature. 50 μl of Griess reagent (2% sulfanilamide, 0.2% *N*-(1-naphthyl)ethylenediamine, 5% phosphoric acid) was then added to 150-μl reaction aliquots, and the absorbance at 550 nm was read after 5 min. Nitrite concentration was determined against a sodium nitrite standard from 0 to 65 μM. The background signal was due to dimer formation that occurred during the 30-min incubation with NOS monomer that was not incubated with arginine during the initial 2.5-h step.

Gel Filtration Chromatography—Gel filtration chromatography of dimerization assay aliquots was performed on a Superdex 200 3.2/30 column using the Amersham Biosciences SMART system. 50-μl aliquots of dimerization mix after 2.5 h of incubation at 37 °C, prepared as described above except using 3 μM iNOS monomer, 2 μM calmodulin, and 1.5 μM hemin, were loaded on the column and chromatographed at 40 μl/min in PBS (25 mM sodium phosphate, 150 mM NaCl, pH 7.2.).

Synthesis of Radioligand—[^{3}H]Compound **3** was synthesized by reaction of Compound **1** with *N*-succinimidyl [2,3-^{3}H]propionate (see Fig. 1*B*). 0.5 ml of *N*-succinimidyl [2,3-^{3}H]propionate (100 Ci/mmol) in toluene was evaporated to dryness in a Speed Vac Concentrator (Savant), after which 20 μl of 100 mM Compound **1** in Me_2SO containing 1 mM HCl was added to the dry tube, followed by 300 μl of 40 mM Bistris propane, pH 7.8. The sample was incubated for 1 h at room temperature and then stored at −80 °C. To remove unreacted Compound **1,** 150 μl of the sample was loaded on a Column Engineering Reliasil C18 HPLC column (300 A, 250 × 4.6 mm). [^{3}H]Compound **3** was eluted after a 5-min column wash using 0.1% trifluoroacetic acid in water (Buffer A) with a 0–50% gradient of 0.1% trifluoroacetic acid in 100% acetonitrile (Buffer B) at a flow rate of 1.0 ml/min. 1.0-ml fractions were collected; [^{3}H]Compound **3** eluted in fractions 36 and 37 and unreacted Compound **1** eluted in fractions 27–30. After concentration 10-fold by drying in a Speed Vac, followed by dilution to 1 ml with 40 mM Bistris propane, pH 7.8, fractions containing the product were pooled and then rechromatographed to further remove unreacted succinimide ester. The specific activity of [^{3}H]Compound **3** product was assumed to be 100 Ci/mmol based on the 1:1 stoichiometry of the reaction.

Competitive Radioligand Binding Assay—0.2 nM [^{3}H]Compound **3** and 4.6 nM full-length human iNOS monomer or 2.2 nM Δ114-iNOS-ox were incubated in the presence of 0–100 μM unlabeled compound in NOS assay buffer. After 60 min at 37 °C, 1-ml aliquots were vacuum-filtered through a PVDF membrane in a 96-well plate format. Before filtration, the PVDF membrane was prepared by presoaking briefly with, successively, 100, 75, 50, and 25% ethanol, followed by water and 45 mM Bistris propane, pH 7.8. Each well of the filter plate was then washed three times with 350 μl of 45 mM Bistris propane, pH 7.8, and after addition of 50 μl of Microscint 20 to each well, the plates were counted in a Wallac Microbeta scintillation counter. Bound radioactivity (counts/min) was plotted *versus* the concentration of unlabeled inhibitor. Apparent K_d values were determined by Scatchard analysis using the program Ligand (National Institutes of Health). The time course of radioligand binding was performed as above, but without the addition of unlabeled compound.

Dissociation Kinetics—0.2 nM [^{3}H]Compound **3** and 4.6 nM human iNOS monomer were incubated for 60 min at 37 °C, after which 100 μM unlabeled Compound **3** was added. At various time points aliquots were removed and filtered through a PVDF membrane, washed, and counted as described above.

Cell-based Assays—The cell-based assay using A-172 human glioblastoma cells was performed as described (30). Briefly, A-172 cells were seeded in 96-well plates at 10^5 cells/well. After overnight incubation, iNOS expression was initiated by the addition of induction medium containing 200 units/ml interferon-γ, 20 ng/ml tumor necrosis factor-α, and 2 ng/ml interleukin 1-β. Nitrite accumulation in cell culture supernatants was measured 24 h later by the addition of Griess reagent, followed by measuring the absorbance at 550 nm. Inhibitors were added at the time of cytokine induction. For the experiments in Table I, induction medium also included 0 to 200 nM Compound **2** (3-fold dilution series), 0.4 or 1.4 mM arginine and/or 1 or 10 μM sepiapterin (an H_4B precursor) as indicated.

Spectral Studies—UV-visible spectra were recorded at room temperature on a Hewlett-Packard HP8452A spectrophotometer using 0.4-ml sample volumes in quartz cuvettes with 1 cm path-length. iNOS monomer isolated from murine macrophage (RAW264.7) cells was used because it had a higher heme content than human iNOS monomer preparations, having been prepared by the dissociation of dimeric iNOS using urea. Full-length murine iNOS monomer at 2 μM was placed in a cuvette, and the spectrum from 350 to 500 nm was measured. The spectrum was taken before and 10 min after addition of 10 μM Compound **2**. Inhibitor binding resulted in a decrease in absorbance at 400 nm and an increase at 428 nm.

RESULTS

Dimerization Assay Using Purified iNOS Monomers—Fig. 1 shows the structures of the compounds used in the present study. The potent and selective pyrimidineimidazole-based inhibitors of iNOS dimerization were discovered using a cell-based assay and found not to inhibit the enzymatic activity of purified dimeric iNOS (30). To study dimerization of iNOS in a purified system, slight modifications of the method described by Baek *et al.* (18) were used, in which active dimeric iNOS was

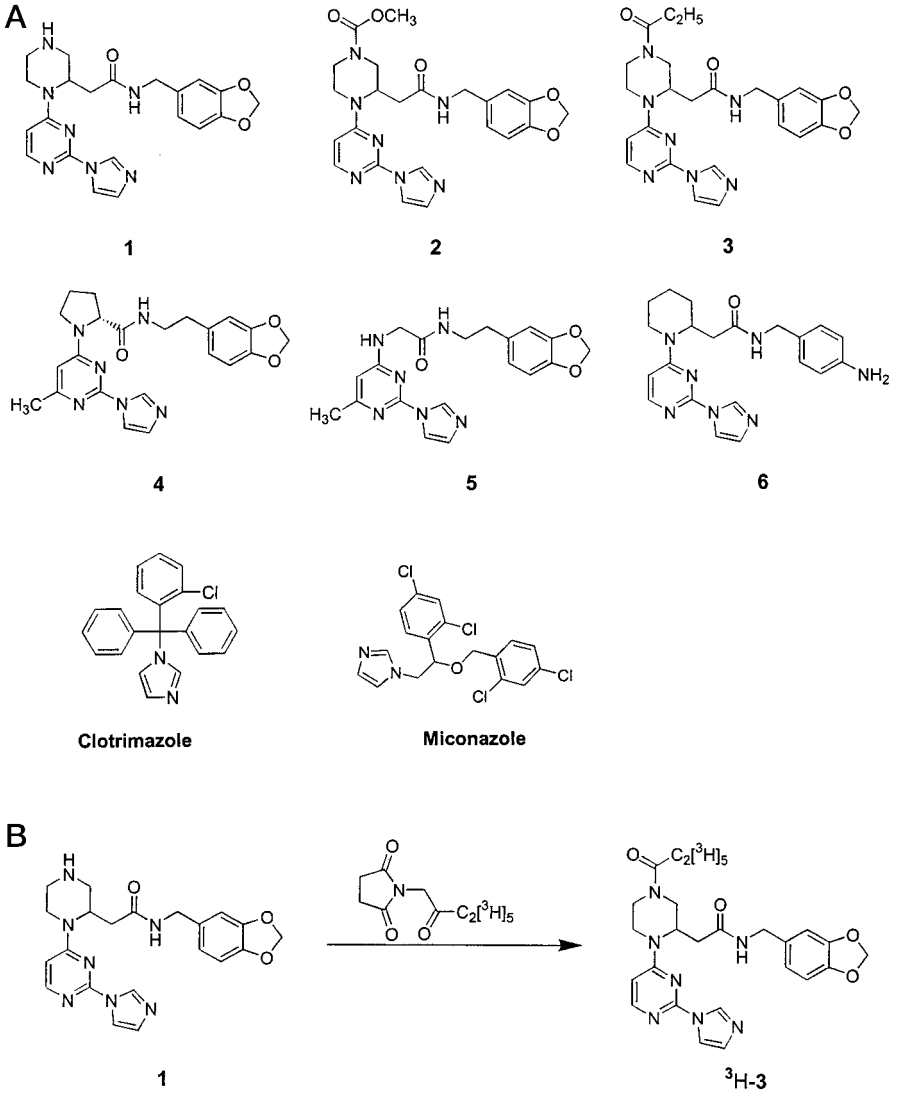

FIG. 1. **Structures of pyrimidineimidazoles and antifungal imidazoles.** *A,* the structures of six pyrimidineimidazoles and the antifungal imidazoles clotrimazole and miconazole are shown. *B,* synthesis of [^{3}H]Compound **3** by reaction of Compound **1** with *N*-succinimidyl [2,3-^{3}H]propionate.

formed after addition of H_4B, arginine, and heme to purified iNOS monomers. Purified full-length human iNOS monomers were incubated with 5 mM arginine in the presence of 4 μM H_4B, with 1.2 μM calmodulin and 0.6 μM hemin added as potential dimer stabilizers. Active dimer formation reached a maximum after 2.5 h at 37 °C (Fig. 2*A*), with NO synthesis measured using the Griess assay. Dimerization was confirmed by gel filtration chromatography on Superdex 200 (Fig. 2*B*).

The time course of dimerization with human full-length iNOS monomers (Fig. 2*A*) correlates well with studies of murine iNOS monomers reported by Baek *et al.* (18). Generation of active dimeric human iNOS was concentration-dependent, with 0.6 μM monomer forming enough dimeric iNOS activity to measure using the Griess reagent, and with concentrations less than 0.1 μM not giving an appreciable signal (data not shown). Fig. 2*B* shows that the starting iNOS monomer preparation contained less than 5% dimeric iNOS (*panel 1*) despite the presence of 4 μM H_4B during isolation. Incubation of monomeric iNOS for 2.5 h at 37 °C with H_4B, but without arginine, produced minimal dimeric NOS (*panel 2*). However, when arginine was added, a significant amount of dimeric iNOS was produced (*panel 3*). The enzymatic activity increased as dimeric NOS was formed, and this activity was inhibited by 2 μM Compound **2** added at the start of the dimerization reaction (Fig. 2*C*). These results with isolated iNOS monomers confirm previous results in cell cultures where treatment of cytokine-stimulated cells with Compound **2** led to accumulation of intracellular monomers (30). Dimerization of human iNOS monomers occurred with or without the addition of heme or calmodulin (Fig. 3). Similar data were obtained with purified full-length murine iNOS monomers (data not shown).

Inhibition of iNOS in Cell-based Assays—Crystallography studies indicate that inhibitor binding prevents formation of the arginine- and H_4B-binding sites in the iNOS monomer by perturbing the monomer structure (30). These results suggest the formation of an inactive inhibitor-monomer complex that should not be prevented or reversed by arginine and H_4B. To test this hypothesis, the effect of arginine and H_4B supplementation in cell-based assays on the IC_{50} of Compound **2** was examined. Cytokine-stimulated A-172 cells were treated with 0–200 nM Compound **2,** and inhibition of NO production was measured at 24 h in the presence of 0.4 mM arginine. As shown in Table I, sepiapterin added at 1 and 10 μM to the medium resulted in very modest increases in the observed IC_{50} for Compound **2** (18 and 40%, respectively). 10 μM sepiapterin resulted in a reproducible but slight increase in NO production in A-172 cells (15%, data not shown), consistent with H_4B being limiting for NO production in this cell type as for other cells. The IC_{50} was not altered by additional arginine (1.4 mM final concentration) in the culture medium (Table I). These results are consistent with those shown in Fig. 2*C* and suggest that Compound **2** inhibits dimerization by a process that is com-

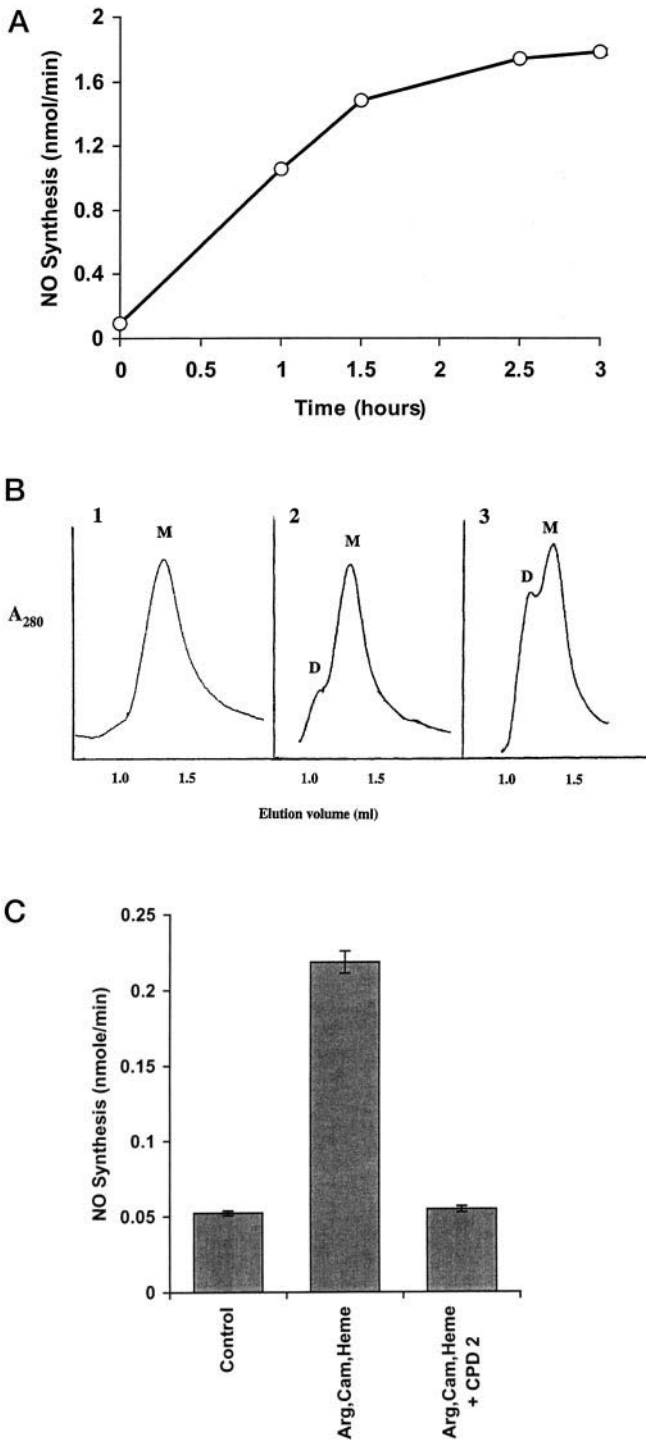

FIG. 2. **Dimerization of human iNOS is prevented by a pyrimidineimidazole.** The *in vitro* dimerization assay was used to measure the increase in NO synthesis activity of human iNOS (H_4B was present in all samples.) *A,* time course of dimerization: 0.6 μM human iNOS monomer was incubated at 37 °C with arginine, calmodulin, and heme. Aliquots were removed at the times indicated and assayed for enzyme activity. *B,* gel filtration profiles: 3 μM iNOS monomer was incubated in the dimerization assay. *D* and *M* indicate dimeric and monomeric iNOS, respectively. *Panel 1*, iNOS monomer before incubation at 37 °C. *Panels 2* and *3*, incubation for 2.5 h at 37 °C without (*panel 2*) and with (*panel 3*) arginine, calmodulin, and heme. *C,* inhibition of dimer formation by a pyrimidineimidazole. NO synthesis activity of 0.6 μM iNOS monomer incubated for 2.5 h at 37 °C without additions (*control*) or with added arginine, calmodulin, and heme (*Arg,Cam,Heme*) in the presence or absence of 2 μM Compound **2.** Data shown in *A* and *C* are mean ± S.D. of triplicate samples and are each representative of three experiments. *A*, the *error bars* are smaller than the symbols. Data in *B* are representative of two experiments.

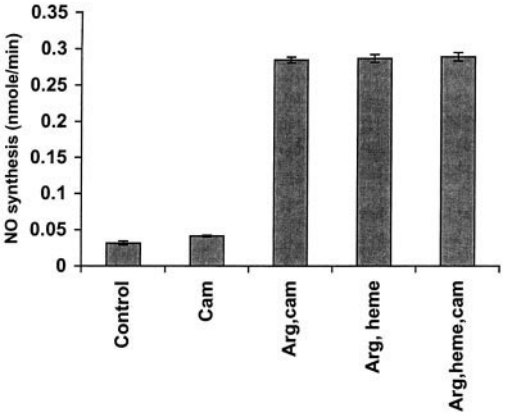

FIG. 3. **Human iNOS monomers require arginine but not additional calmodulin or heme to dimerize.** NO synthesis activity of 0.6 μM human iNOS monomer incubated in the dimerization assay for 2.5 h at 37 °C with arginine, calmodulin (*Cam*), and/or heme as indicated. (H_4B was present in all samples.) Data shown are mean ± S.D. from triplicate samples and are representative of two independent experiments.

TABLE I
Effect of added arginine or sepiapterin (an H_4B precursor) on IC_{50} of Compound 2 in the A-172 cell-based assay

Data shown are mean ± S.D. of IC_{50} determinations from $n = 3$ experiments.

[Arginine]	[Sepiapterin]	IC_{50}
mM	*μM*	*nM*
0.4	0	2.2 ± 0.15
0.4	1	2.6 ± 0.11
0.4	10	3.1 ± 0.10
1.4	0	2.4 ± 0.80

pletely independent of arginine and minimally affected by H_4B. This contrasts to other iNOS inhibitor classes that are based on the substrate L-arginine or the cofactor H_4B.

A-172 cells were also treated with 5 μM Compound **2** at various time points *after* the addition of interferon-γ, tumor necrosis factor-α, and IL1-β. The extent of inhibition decreased with time, starting at about 6 h after induction, with little or no inhibition seen when the compound was added 24 h after induction (data not shown). This observation has been confirmed by similar experiments with J774.1 murine macrophage cells.[2] As Compound **2** does not inhibit preformed, active dimer, the cell-based assay results suggest that the compounds did not act by dissociating dimeric NOS but by preventing the association of iNOS monomers.

Competitive Radioligand Binding Assay—Fig. 1*B* shows the reaction of Compound **1** with *N*-succinimidyl [2,3-^{3}H]propionate to provide the radiolabel, [^{3}H]Compound **3**. This facile synthesis yielded a radiolabeled compound with a specific activity of ~100 Ci/mmol. The incorporation of radiolabel at the secondary nitrogen of the piperazine ring was selected on the basis of structure-activity relationships in the A-172 cell-based assay, which showed that this region was not essential for inhibitor activity.[3] This was subsequently confirmed by x-ray crystallographic data showing that this region of the inhibitor is exposed to solvent and not involved in iNOS monomer-inhibitor binding interactions (30).

[^{3}H]Compound **3** was used to develop a rapid filtration competitive radioligand-binding assay to measure direct binding affinities of compounds to monomeric iNOS. In the assay, the

[2] D. Ghosh, personal communication.
[3] M. A. Polokoff, G. B. Phillips, and J. F. Parkinson, unpublished observations.

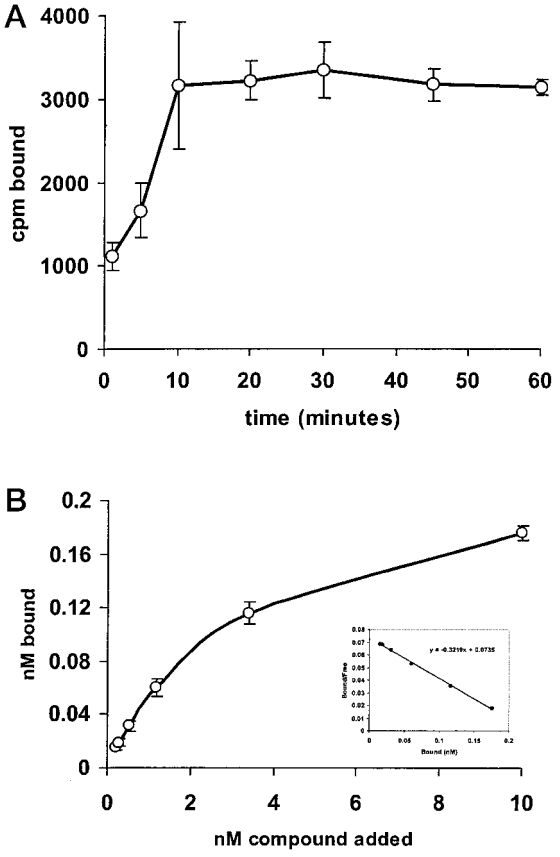

FIG. 4. **Rapid filtration radioligand binding assay using human iNOS monomer.** *A,* time course. 4.6 nM human iNOS monomer was incubated with 0.2 nM [^{3}H]Compound **3** at 37 °C. At the times indicated, reactions were filtered through a PVDF membrane to remove unbound radioligand, and after washing, bound radioactivity was measured using a scintillation counter (see "Experimental Procedures"). *B,* competition binding. 4.6 nM human iNOS monomer was incubated with 0.2 nM [^{3}H]Compound **3** and 0–10 nM cold Compound **3** for 1 h at 37 °C, followed by filtration and counting as described under "Experimental Procedures." The linear Scatchard plot (*inset*) gave apparent K_d = 2.5 and 0.19 nM total binding sites. Data in both *A* and *B* are mean ± S.D. of six replicate points within the same experiment. Data are representative of three experiments.

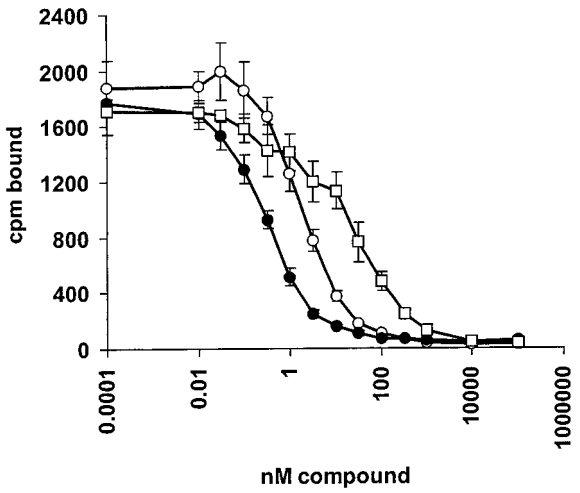

FIG. 5. **Competitive binding of three pyrimidineimidazoles in the binding assay.** Competition binding was performed as described in Fig. 4 using 0–100 μM Compound **3** (*open circles*), **5** (*filled circles*) and **6** (*open squares*) as competing ligand. Scatchard analyses gave apparent K_d values of 1.8, 0.33, and 27 nM, respectively. Data are mean ± S.D. of six replicate points within the same experiment. Data for compounds **3, 5,** and **6** are representative of 4, 3, and 1 experiment, respectively.

amount of iNOS monomer added was sufficient to bind about 2000 cpm, or 10% of the available radioligand. The binding reaction volume was increased from 0.1 to 1.0 ml in deep-well microtiter plates to maximize sensitivity by lowering the concentration of iNOS monomer. Fig. 4 shows that binding reached equilibrium within 30 min. The Scatchard analysis is linear and fits a one-site binding model with apparent K_d = 2.5 nM for Compound **3** (mean 1.80 ± 0.45 nM, n = 4). The concentration of binding sites by Scatchard analysis was 0.19 nM or about 4% of the total monomer concentration. This correlates roughly with the low heme content (about 10%) and is consistent with the hypothesis that compounds bind to heme-containing NOS monomers.

Binding of related compounds was measured by competition against [^{3}H]Compound **3**. Compounds were added to purified iNOS monomer at concentrations ranging from 0 to 100 μM along with 0.2 nM [^{3}H]Compound **3**. Fig. 5 shows that the assay can distinguish between compounds of binding affinities of 0.33, 1.8, and 27 nM. Both this assay and the dimerization assay were performed in the presence of 4 μM H_4B, which did not prevent compound binding. The compounds also bound monomeric murine iNOS oxygenase domain lacking the first 114 N-terminal residues (Δ114-iNOS-ox). Fig. 6 shows the competition of [^{3}H]Compound **3** by Compound **4** with Δ114-iNOS-ox. High affinity binding was observed with apparent K_d = 6.25 ± 3.5 nM (n = 4). Because Δ114-iNOS-ox does not bind H_4B (8, 28, 30), the results support the finding in cell-based assays (see above) that the compounds can bind iNOS monomers in an H_4B-independent manner.

Table II summarizes the relationship between affinity (apparent K_d) to purified human iNOS monomers in the binding assay and potency (IC_{50}) in the cell-based assay for human iNOS in cytokine-stimulated A-172 cells. Compounds with apparent K_d values in the pM to nM range typically had IC_{50} values in the same range in the cell-based assay. The lack of an absolute correlation may reflect several factors. The concentration of iNOS monomers is likely to be higher in the binding assay than in the cell-based assay. In addition, the binding assay is a static system, whereas in cells the iNOS monomers are in equilibrium with iNOS dimers. The cellular system may also introduce subtle differences due to compound permeability and intracellular compartmentalization. The antifungal imidazoles miconazole and clotrimazole, which were previously reported to inhibit iNOS dimerization (40), were active in both assays, but with much lower potency than the pyrimidineimidazoles. The iNOS heme ligand imidazole was competitive with [^{3}H]Compound **3,** confirming that heme ligation is key to the binding affinity of these compounds. The affinity for binding of imidazole to iNOS monomers determined by this method, apparent K_d = 42 μM, is similar to the IC_{50} (200 μM) of imidazole in iNOS enzyme inhibition assays and the spectral binding constant with purified iNOS (K_s ~160 μM), as reported previously (14, 22). The slightly higher imidazole affinity measured in the binding assay is likely a result of assay sensitivity and the fact that much lower NOS protein concentrations were used.

Off and On Rates of Radioligand—The rate of dissociation of [^{3}H]Compound **3** from human iNOS monomers was measured at 22 °C (not shown) and at 37 °C after adding 100 μM excess cold Compound **3** (Fig. 7). The $t_{1/2}$ was 201 min at 22 °C and 93 min at 37 °C. From this the K_{off} was calculated to be 5.8×10^{-5} s^{-1} at 22 °C and 1.2×10^{-4} s^{-1} at 37 °C. As the apparent K_d is 2 nM, the K_{on} is calculated to be 6×10^4 M^{-1} s^{-1} at 37 °C. This calculated on-rate is similar to that reported for the binding of CO to iNOSox at 10 °C (K_{on} = 10^4 to 10^5 M^{-1} s^{-1}) but is lower

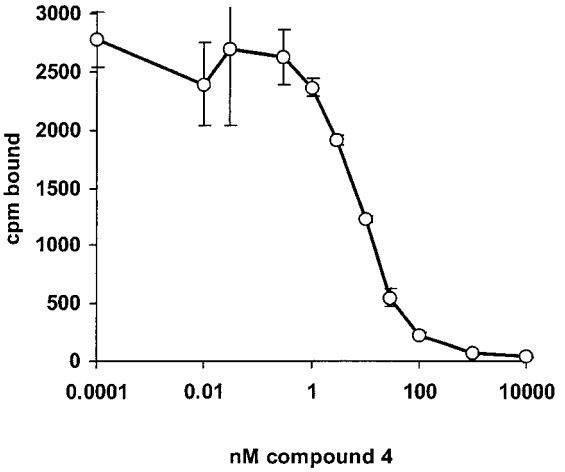

FIG. 6. **Pyrimidineimidazoles bind murine Δ114-iNOS-ox monomer with high affinity.** Competition binding was performed as described in Fig. 4 using 0.2 nM [^{3}H]Compound **3,** 2.2 nM murine Δ114-iNOS-ox monomer, and 0–100 μM Compound **4** as competing ligand. Apparent K_d = 10 nM. Data are mean ± S.D. of six replicate points within the same experiment; the graph is representative of four experiments.

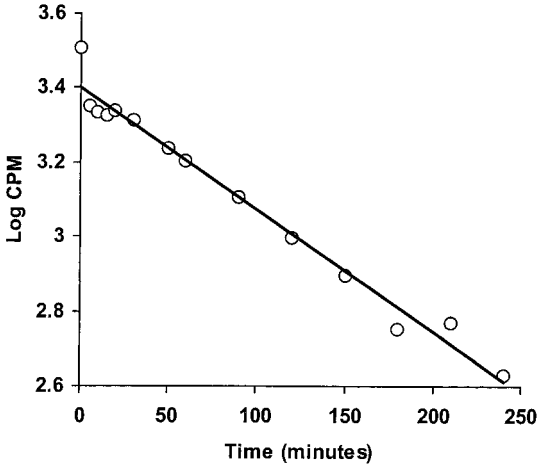

FIG. 7. **Dissociation kinetics of [^{3}H]Compound 3 from human iNOS monomer.** 0.2 nM [^{3}H]Compound **3** and 4.6 nM human iNOS monomer were incubated for 60 min at 37 °C, after which 100 μM excess cold Compound **3** was added. At various time points aliquots were removed and filtered through a PVDF membrane, washed, and counted as described under "Experimental Procedures." A dissociation half-life of 93 min provided a calculated K_{off} = 1.2. × 10^{-4} s^{-1} and K_{on} = 6 × 10^4 M^{-1} s^{-1} for Compound **3**. Data are mean of six replicate points within one experiment. The S.E. for each data point was less than 10%.

TABLE II

Correlation between binding affinity to iNOS monomers (apparent K_d) and inhibitory potency in the iNOS cell-based assay (IC_{50}) for imidazole-containing compounds

Affinity to purified human iNOS monomers was measured using the radioligand binding assay, and inhibition of human iNOS was measured in cytokine-stimulated A-172 cells, as described under "Experimental Procedures." Apparent K_d values are mean ± S.D. of values obtained from each individual experiment.

Compound	Radioligand binding assay apparent K_d	A-172 cell-based assay IC_{50}
	nM	*nM*
1	0.73 ± 0.13, *n* = 2	0.50 ± 0.29, *n* = 6
2	2.2 ± 0.28, *n* = 2	0.74 ± 0.76, *n* = 21
3	1.8 ± 0.45, *n* = 4	0.38 ± 0.15, *n* = 3
4	0.09 ± 0.02, *n* = 3	0.49 ± 0.30, *n* = 116
5	0.33 ± 0.20, *n* = 3	1.20 ± 0.61, *n* = 3
6	27, *n* = 1	270, *n* = 2
Miconazole	6000, *n* = 1	>10,000[a]
Clotrimazole	2500, *n* = 1	2800
Imidazole	42000, *n* = 1	Not determined

[a] 5% inhibition at 10 μM.

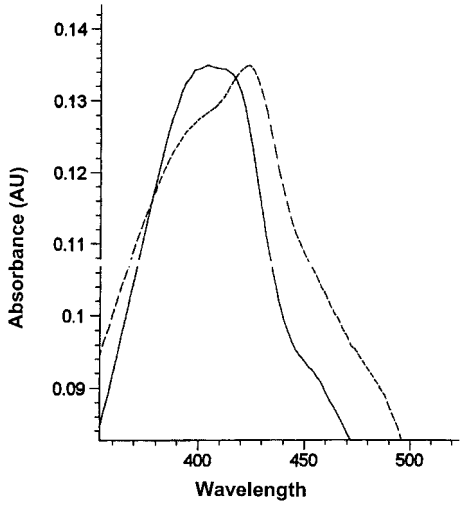

FIG. 8. **Binding of a pyrimidineimidazole to murine iNOS monomer causes a shift of the heme iron to the low spin state.** Absorbance spectrum of 2 μM murine iNOS monomer before (*solid line*) and after (*dotted line*) incubation with 10 μM Compound **2**. The spectral shift to an absorbance maximum at 428 nm indicates a shift of the heme iron to the low spin state and is similar to that seen with imidazole binding. Data are representative of two individual experiments.

than that reported for imidazole binding to eNOS at 24 °C (1 × 10^6 M^{-1} s^{-1}) (35, 36). The results suggest that the binding of the pyrimidineimidazole inhibitors to iNOS monomers is reversible and that a slow off-rate is the principal determinant of high affinity binding.

Changes in Absorbance Spectra Due to Compound Binding—Spectral studies (Fig. 8) show that like imidazole, the pyrimidineimidazole inhibitors cause a shift of the heme iron of murine iNOS monomer to a low spin state (absorbance maximum at 428 nm), which is characteristic of binding to the iron as a sixth ligand (37).

DISCUSSION

Novel pyrimidineimidazole-based iNOS inhibitors previously identified using a cell-based assay (30) are shown here to inhibit dimerization of purified iNOS monomers. In addition, a high affinity radiolabeled inhibitor was used to develop a rapid filtration binding assay using purified human and murine iNOS monomers. This binding assay had a broad dynamic range, allowing for inhibitor affinities to be measured in the pM to μM range and also exhibited good correlation with inhibitor potency in the cell-based assay. The biochemical results are consistent with the pyrimidineimidazoles forming a high affinity complex with iNOS monomers via heme ligation, as evidenced by spectral perturbations and competition with the known iNOS heme ligands imidazole, clotrimazole, and miconazole.

Although human iNOS monomer/dimer ratios have been studied in cell lysates (38, 39), the present work is the first to describe human iNOS dimer formation from purified iNOS monomers. The results are thus discussed relative to published studies with murine iNOS monomers. During purification, the mammalian cell-expressed human iNOS monomers were separated from dimeric iNOS using gel filtration chromatography, in the presence of 4 μM H_4B at 4 °C, and were stored frozen immediately after elution from the column. Despite the presence of 4 μM H_4B, the iNOS monomer preparation contained little dimeric iNOS at the start of the *in vitro* dimerization

assay, and little active iNOS dimer was formed in the presence of H_4B alone. Thus, the substrate L-arginine rather than H_4B appeared to promote human iNOS dimerization under the conditions used. As shown in Fig. 2*B*, not all of the human iNOS monomers could be dimerized even in the presence of excess arginine, H_4B, heme, and calmodulin. The data are consistent with the human iNOS monomer preparations containing a mixture of heme-bound (~10%) and heme-free (~90%) species and that only the heme-bound species is capable of dimerizing. An implication of these findings is that a large proportion of the recombinant human iNOS monomers isolated from cells have no bound heme and cannot bind exogenously added heme. These are likely to be denatured species that cannot dimerize. The murine iNOS monomer used in the present studies, which was prepared by dissociation of dimeric iNOS with urea, does not require added heme to dimerize, in contrast to results published previously (18) using monomers isolated directly from mouse macrophage cells. As the murine iNOS monomer preparation is already 95% heme-containing (see "Experimental Procedures"), a requirement for added heme to promote dimerization would not be expected.

In relation to time course, arginine- and H_4B-dependence, the results with human iNOS are comparable with previous studies using full-length murine iNOS monomer (18) and murine iNOS oxygenase domain monomer (24). In these studies, dimerization was minimal with the addition of H_4B alone as compared with the addition of both H_4B and arginine. However, in other studies using murine iNOS oxygenase domain (28, 41) or full-length iNOS monomers (41), the extent of dimerization observed with H_4B alone was about 50% (28) to over 80% (41) that seen with both H_4B and arginine. These disparate results may reflect differences in the procedures for monomer isolation.

The affinity and reactivity of pyrimidineimidazoles with human and murine iNOS are distinct from imidazole-containing iNOS reported previously. The novel compounds used in this study (see Fig. 1) are derivatized pyrimidineimidazoles with a bulky side chain that interacts with the iNOS monomer at a separate site from the imidazole-heme interaction (30). Smaller compounds, such as imidazole, 1-phenylimidazole, and 7-nitroindazole, actually promote dimerization (40). Unlike the pyrimidineimidazoles described here, all of these smaller compounds inhibit the activity of dimeric iNOS (14). The heme iron of iNOS monomers can bind large 1-substituted imidazoles with affinity in the micromolar range, consistent with the observation that iNOS monomers contain a relatively open distal heme pocket. The antifungal imidazoles clotrimazole and miconazole prevent iNOS dimerization (40), presumably due to steric hindrance from the aromatic side chains (Fig. 1). The 1000-fold higher affinity of the pyrimidineimidazoles for iNOS monomers over clotrimazole and miconazole is presumably due to specific interactions with residues in the iNOS monomer. The crystal structure of Compound **2** bound to monomeric Δ114-iNOS-ox (30) reveals that the free imidazole nitrogen coordinates directly to the heme, and the benzodioxolane group makes specific contacts with the iNOS monomer, thereby disrupting the arginine-binding site. Compound **2** also disrupts helix 7a and helix 8, which are part of the iNOS dimer interface. These findings predict the formation of a dead-end inhibitor complex that should not be prevented by excess arginine or H_4B in cell culture medium. IC_{50} determinations for Compound **2** in the cell-based assays confirm this hypothesis.

A general model for iNOS dimer assembly and its inhibition by these compounds is shown in Fig. 9 and is similar to that proposed for the effects of antifungal imidazoles on murine iNOS (40). Heme insertion is the first step in dimerization (18, 19, 42). Binding of heme leads to the formation of a loosely formed dimer (Fig. 9, *DIMER-Fe*) which then binds H_4B and arginine to form a stable, compact enzymatically active dimer (Fig. 9, *DIMER-Fe-H$_4$B-Arg*). The pyrimidineimidazoles do not inhibit the activity of dimeric iNOS even after prolonged incubation (IC_{50} >100 μM).[3] In addition, spectral binding experiments with purified iNOS confirm high affinity binding to iNOS monomers (K_s < =50 nM) but low affinity binding to iNOS dimers (K_s > 10 μM).[2] The correlation between human monomer heme content and inhibitor binding sites from Scatchard analysis indicates that inhibitors do not bind to heme-free, but rather to heme-containing, iNOS monomers. Thus, in cells, these inhibitors act by binding to a transient species that, in the absence of compound, would rapidly dimerize. In the presence of compound, monomeric iNOS is trapped in a nonfunctional monomer-heme-inhibitor complex. An implication of our findings is that in cell culture systems the equilibrium between the heme-containing monomer species and the dimer is in favor of the dimer and that once stable iNOS dimers are formed there is little dissociation back to monomers. This is supported by the finding that iNOS monomer isolated from murine macrophages is heme-free, whereas all heme-containing iNOS is dimeric (18). The ability of the pyrimidineimidazoles to bind and destabilize the proposed "loose" iNOS dimer that is H_4B- and arginine-free, remains to be determined.

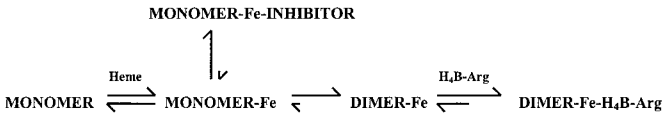

FIG. 9. **Model for inhibition of iNOS dimer assembly by pyrimidineimidazoles.** The model shows the progress from iNOS monomers to active iNOS dimer with bound L-arginine and H_4B. Heme insertion initiates dimerization. Pyrimidineimidazoles bind to the transient heme-containing monomer species and form an inactive monomer-heme-inhibitor complex. Due to the loss of inhibition of iNOS in cells when dimerization inhibitors are added >6 h after cytokine stimulation, it is proposed that there is little reversible equilibrium to iNOS monomer once iNOS dimer has formed.

Previously the pyrimidineimidazoles were shown to exhibit high selectivity (>1000-fold) for inhibiting iNOS *versus* eNOS dimerization, whereas the selectivity ratio for nNOS was only ~5-fold for Compound **2** (30). High eNOS selectivity is retained for all of the pyrimidineimidazoles shown in Fig. 1, whereas nNOS selectivity ranges from 5- to 100-fold and is altered by changing the substituents on the pyrimidineimidazole core.[3] These results indicate that the compounds exhibit specific affinity for the iNOS and nNOS monomers but may not have appreciable affinity for eNOS monomers. The molecular basis for this isoform selectivity is not readily apparent from analysis of the crystal structures of the active sites of the NOS isoforms.

It is also noted that there is an inverse relationship between the stability of the iNOS, nNOS, and eNOS dimers and the isoform selectivity of these pyrimidineimidazoles. It is reported that eNOS dimers are the most stable, nNOS next, and iNOS dimers the least stable, as measured by dimer resistance to chaotropes such as urea or SDS (42–44). Thus, in addition to binding specificity, the NOS isoform selectivity may be partially explained by considering the energetics that drive NOS monomer-dimer equilibria. With the other isoforms relative to iNOS, the free energy difference between heme-containing monomer and dimer is larger, and thus the steady state monomer-dimer equilibrium progresses in favor of dimer formation in the order eNOS ≫ nNOS > iNOS. In a competition between the formation of dimer and the formation of a monomer-inhibitor complex, the amount of inhibitor required to effectively compete is dependent upon this equilibrium and therefore is much greater for eNOS than nNOS or iNOS. It is thus formally

possible that the inhibitors have appreciable affinity for eNOS monomers, but inhibition is not observed due to the eNOS monomer-dimer equilibrium. The model also predicts that the set point for the eNOS monomer ↔ dimer equilibrium is very heavily in favor of eNOS dimer and that the transient eNOS monomer species with bound heme will be very difficult to isolate. This is consistent with repeated unsuccessful attempts to isolate native heme-containing eNOS monomers using chaotropes that readily provide iNOS and nNOS monomers.[4]

Regarding the general pharmacological selectivity of the pyrimidineimidazoles, extensive receptor and enzyme selectivity tests have been performed with compounds from the series. Compound **4** has broad pharmacological selectivity in such assays with $IC_{50} > 10–100$ μM and is not cytotoxic.[3] Imidazole-containing compounds are known to bind and inhibit cytochromes P450, and interaction with the major metabolizing enzyme CYP-3A4 is potentially problematic. For the pyrimidineimidazoles, cross-reactivity with CYP-3A4, but not other drug-metabolizing P450s, was observed, with a range of potencies depending on chemical substituents.[3] The IC_{50} of Compound **4** for CYP-3A4 is ~150 nM in a microsomal benzyloxyresorufin assay and ~1 μM in a cell-based testosterone hydroxylase assay. Compound **4** is thus ~300–2000-fold selective for inhibiting iNOS dimerization in cells *versus* CYP-3A4. As reported previously (30), Compound **4** is more potent in cell culture systems than any other currently known substrate- or pterin-based iNOS inhibitor. In summary, Compound **4** is a highly selective, potent, and cell-permeable research tool that can be used to inhibit specifically iNOS and study its cellular function.

The availability of high affinity inhibitors as reported here may be useful in further understanding iNOS dimerization, in both protein-based and cellular systems. [^{3}H]Compound **3** accumulates in cells induced to express iNOS by cytokines, presumably by binding to iNOS monomers synthesized within the cell.[5] Pulse-chase experiments could thus explore the relationship between heme incorporation into iNOS, which may occur co-translationally, and radiolabel incorporation. In addition, dimerization inhibitors could be used to examine the fate of iNOS monomers within cells. It has been shown recently that nNOS monomers are preferentially ubiquitinated and degraded by the proteasome pathway (45). Caveolin-1 expression in HT29 and DLD-1 cells targets iNOS for proteasomal degradation (46), and the proteasome pathway degrades both human iNOS dimers and monomers when expressed in 293 cells (47). The effect of iNOS dimerization inhibitors on these processes should be examined because inhibitor-induced proteasomal degradation of iNOS monomers may be a desirable property and contribute to the therapeutic potential of this class of inhibitors. Because of their mode of action and high potency, these novel compounds can be useful tools for new studies elucidating the cellular synthesis and degradation of the iNOS enzyme.

Acknowledgments—We gratefully thank Rhonda Humm for cell culture work and Vivien Lee for assistance on the radioligand binding assay.

REFERENCES

1. Marletta, M. A. (1994) *Cell* **78,** 927–930
2. Griffith, O. W., and Stuehr, D. J. (1995) *Annu. Rev. Physiol.* **57,** 707–736
3. Masters, B. S. S., McMillan, K., Sheta, E. A., Nishimura, J. S., Roman L. J., and Martasek, P. (1995) *FASEB J.* **10,** 552–558
4. Bredt, D. S., Hwang, P. M., Glatt, C. E., Lowenstein, C., Reed, R. R., and Snyder, S. H. (1991) *Nature* **351,** 714–718
5. Ghosh, D. K., and Stuehr, D. J. (1995) *Biochemistry* **34,** 801–807
6. Klatt, P., Schmidt, K., and Mayer, B. (1992) *Biochem. J.* **288,** 15–17
7. McMillan, K., Bredt, D. S., Hirsch, D. J., Snyder, S. H., Clark, J. E., and Masters, B. S. S. (1992) *Proc. Natl. Acad. Sci. U. S. A.* **89,** 11141–11145
8. Crane, B. R., Arvai, A. S., Ghosh, D. K., Wu, C., Getzoff, E. D., Stuehr, D. J., and Tainer, J. A. (1998) *Science* **279,** 2121–2126
9. Abu-Soud, H. M., Gachhui, R., Raushel, F. M., and Stuehr, D. J. (1997) *J. Biol. Chem.* **272,** 17349–17353
10. Pufahl, R. A., and Marletta, M. A. (1993) *Biochem. Biophys. Res. Commun.* **193,** 963–970
11. Nishimura, J. S., Martasek, P., McMillan, K, Salerno, J. C., Liu, Q., Gross, S. S., and Masters, B. S. S. (1995) *Biochem. Biophys. Res. Commun.* **210,** 288–294
12. Sari, M. A., Booker, S., Jaouen, M., Vadon, S., Boucher, J. L., Pompon, D., and Mansuy, D. (1996) *Biochemistry* **35,** 7204–7213
13. Chen, P. F., Tsai, A. L., and Wu, K. K. (1994) *J. Biol. Chem.* **269,** 25062–25066
14. Wolff, D. J., Datto, Ga. A., Samatovicz, R. A., and Tempsick, R. A. (1993) *J. Biol. Chem.* **268,** 9425–9429
15. Hurshman, A. R., and Marletta, M. A. (1995) *Biochemistry* **34,** 5627–5634
16. Abu-Soud, H. M., Wang, J., Rousseau, D. L., Fukuto, J. M., Ignarro, L. J., and Stuehr, D. J. (1995) *J. Biol. Chem.* **270,** 22997–23006
17. Matsuoka, A., Stuehr, D. J., Olson, J. S., Clark, P., and Ikeda-Saito, M. (1994) *J. Biol. Chem.* **269,** 20335–20339
18. Baek, K. J., Thiel, B. A., Lucas, S., and Stuehr, D. J. (1993) *J. Biol. Chem.* **268,** 21120–21129
19. Klatt, P., Pfeiffer, S., List, B. M., Lehner, D., Glatter, O., Bachinger, H. P., Werner, E. R., Schmidt, K., and Mayer, B. (1996) *J. Biol. Chem.* **271,** 7336–7342
20. Rodriguez-Crespo, I., Gerber, N. C., and Ortiz de Montellano, P. R. (1996) *J. Biol. Chem.* **271,** 11462–11467
21. Venema. R. C., Ju, H., Zou, R., Ryan, J. W., and Venema, V. J. (1997) *J. Biol. Chem.* **272,** 1276–1282
22. McMillan, K., and Masters, B. S. S. (1995*) Biochemistry* **34,** 3686–3693
23. Chen, P. F., Tsai, A. L., Berka, V., and Wu, K. K. (1996*) J. Biol. Chem.* **271,** 14631–14635
24. Ghosh, D. K., Abu-Soud, H. M., and Stuehr, D. J. (1996) *Biochemistry* **35,** 1444–1449
25. Siddhanta, U., Presta, A., Fan, B., Wolan, D., Rousseau, D. L., and Stuehr, D. J. (1998) *J. Biol. Chem.* **273,** 18950–18958
26. Riveros-Morino, V., Heffernan, B., Torres, B., Chubb, A., Charles, I., and Moncada, S. (1995) *Eur. J. Biochem.* **230,** 52–57
27. Stuehr, D. J. (1997) *Annu. Rev. Pharmacol. Toxicol.* **37,** 339–359
28. Ghosh, D. K., Wu, C., Pitters, E., Moloney, M., Werner, E. R., Mayer, B., and Stuehr, D. J. (1997) *Biochemistry* **36,** 10609–10619
29. Abu-Soud, H. M., Loftus, M., and Stuehr, D. J. (1995) *Biochemistry* **34,** 11167–11175
30. McMillan, K., Adler, M., Auld, D. S., Baldwin, J. J., Blasko, E., Browne, L. J., Chelsky, D., Davey, D., Dolle, R. E., Eagen, K. A., Erickson, S., Feldman, R. I., Glaser, C. B., Mallari, C., Morrissey, M. M., Ohlmeyer, M. H. J., Pan, C. H., Parkinson, J. F., Phillips, G. B., Polokoff, M. A., Sigal, N. H., Vergona, R., Whitlow, M., Young, T. A., and Devlin, J. J. (2000) *Proc. Natl. Acad. Sci. U. S. A.* **97,** 1506–1511
31. Deleted in proof
32. Crane, B. R., Arvai, A. S., Gacchui, R., Wu, C., Ghosh, D. K., Getzoff, E. D., Stuehr, D. J., and Tainer, J. A. (1997) *Science* **278,** 425–431
33. White, K. A., and Marletta, M. A. (1992) *Biochemistry* **31,** 6627–6631
34. Stuehr, D. J., and Marletta, M. A. (1985) *Proc. Natl. Acad. Sci. U. S. A.* **82,** 7738–7742
35. Abu-Soud, H. M., Wu, C., Ghosh, D. K., and Stuehr, D. J. (1998) *Biochemistry* **37,** 3777–3786
36. Berka, V., and Tsai, A. (2000) *Biochemistry* **39,** 9373–9383
37. McMillan, K., and Masters, B. S. S. (1993) *Biochemistry* **32,** 9875–9880
38. Tzeng, E., Billiar, T. R., Robbins, P. D., Loftus, M., and Stuehr, D. J. (1995) *Proc. Natl. Acad. Sci. U. S. A.* **92,** 11771–11775
39. Eissa, N. T., Yuan, J. W., Haggerty, C. M., Choo, E. K., Palmer, C. D., and Moss, J. (1998) *Proc. Natl. Acad. Sci. U. S. A.* **95,** 7625–7630
40. Sennequier, N., Wolan, D., and Stuehr, D. J. (1999) *J. Biol. Chem.* **274,** 930–938
41. Presta, A., Siddhanta, U., Wu, C., Sennequier, N., Huang, L., Abu-Soud, H. M., Erzurum, S., and Stuehr, D. J. (1998) *Biochemistry* **37,** 298–310
42. Bender, A. T., Nakatsuka, M., and Osawa, Y. (2000) *J. Biol. Chem.* **275,** 26018–26023
43. Panda, K., Ghosh, S., Adak, S., Meade, A., and Stuehr, D. J. (2000) *Nitric Oxide* **4,** 222
44. Klatt, P., Schmidt, K., Lehner, D., Glatter, O., Bachinger, H. P., and Mayer, B. (1995) *EMBO J.* **14,** 15., 3687–3895
45. Bender, A. T., Demady, D. R., and Osawa, Y. (2000) *J. Biol. Chem.* **275,** 17407–17411
46. Felley-Bosco, E., Bender, F. C., Courjault-Gautier, F., Bron, C., and Quest, A. F. (2000) *Proc. Natl. Acad. Sci. U. S. A.* **97,** 14334–14339
47. Musial, A., and Eissa, N. T. (2001) *J. Biol. Chem.* **276,** 24268–24273

[4] D. J. Stuehr, unpublished observations.
[5] E. Blasko, unpublished observations.